Probabilistic Engineering Mechanics 59 (2020) 103017

Contents lists available at ScienceDirect

Probabilistic Engineering Mechanics

journal homepage: www.elsevier.com/locate/probengmech

Analysis of block random rocking on nonlinear flexible foundation

A. Di Matteo [a,*], A. Pirrotta [a], E. Gebel [b], P.D. Spanos [c]

[a] Department of Engineering, Università degli Studi di Palermo, Palermo, Italy
[b] Department of Automation and Robotics, Omsk State Technical University, Omsk, Russia
[c] L.B. Ryon Chair in Engineering, Department of Mechanical Engineering and Materials Science, Rice University, Houston, TX, USA

ARTICLE INFO

Keywords:
Rocking motion
Nonlinear flexible foundation
Random base excitation

ABSTRACT

In this paper the rocking response of a rigid block randomly excited at its foundation is examined. A nonlinear flexible foundation model is considered accounting for the possibility of uplifting in the case of strong excitation. Specifically, based on an appropriate nonlinear impact force model, the foundation is treated as a bed of continuously distributed springs in parallel with nonlinear dampers. The statistics of the rocking response is examined by an analytical procedure which involves a combination of static condensation and stochastic linearization methods. In this manner, repeated numerical integration of the highly nonlinear differential equations of motion is circumvented, and a computationally efficient semi-analytical solution is obtained. Comparisons with pertinent Monte Carlo simulations demonstrate the efficiency and reliability of the proposed approach. Finally, the survival probability related to toppling of the blocks subject to filtered white noise excitation is investigated, for different kinds of block geometries, foundation materials, and filter parameters.

1. Introduction

Rocking motion, a complex phenomenon related to the behavior of block-like structures allowed to rock due to base excitation has been extensively studied over a period of several decades. In this regard, considerable research efforts have been devoted to determining the rocking response of structures not rigidly connected to their foundations. Representative examples are oil tanks [1]; pieces of machinery [2,3]; and museum exhibits [4] of marble ancient structures [5,6]. Nevertheless, the problem remains technically challenging due to, inter alia, the potential beneficial effects induced by base uplifting occurring during rocking motion, as exploited for the design of several bridges [7–10].

Several alternative analytical models have been proposed to study rocking dynamics. However, two models are primarily used to describe the rocking of rigid bodies subjected to ground motion; they are two-dimensional, and afford a reasonable representation of the phenomenon. The first model, henceforth referred to as the Housner model (HM) [1], deals with the motion of a rigid block rocking about its base corners on a rigid foundation [7,11–14]. In this regard, piecewise analytical solutions have been obtained both for the free-rocking case [15], and for harmonic base excitation [16]. The second model, known as the Winkler foundation model (WFM), deals with the motion of a rigid block rocking on a flexible foundation of distributed linear vertical springs and dashpots [17]. In this regard, several authors have analyzed several aspects of this model, providing results for the case of harmonic and earthquake base excitations [17–19], as well, insight on the coupled effect of sliding and uplifting [20].

Note that, considering the inherent stochastic nature of the seismic excitation, several authors have analyzed the rocking response in case of random base motion, although to a lesser degree with respect to the case of deterministic excitation. Specifically, some analyses considering the HM are reported in [21–27], while some studies considering the WFM can be found in [28,29].

Further, recent studies have pointed out the strong effect of different foundation materials on the rocking dynamics, which may lead in some cases to counterintuitive responses [11,30], especially when flexible foundation materials are employed. In this regard, to better understand this complex phenomenon, as well as to take into account aspects which may arise during the rocking motion of rigid blocks on flexible foundations, recently in [31] a nonlinear model has been used for the base-foundation interaction. Specifically, the Hunt and Crossley nonlinear impact force model [32] has been adopted, and the foundation has been treated as a bed of continuously distributed linear tensionless springs in parallel with nonlinear dampers.

In this paper, based on the aforementioned study, the random rocking response of rigid blocks on the proposed nonlinear foundation model is considered. Specifically, both the cases of time-modulated

* Corresponding author.
E-mail addresses: alberto.dimatteo@unipa.it (A. Di Matteo), antonina.pirrotta@unipa.it (A. Pirrotta), gebel-es@mail.ru (E. Gebel), spanos@rice.edu (P.D. Spanos).

https://doi.org/10.1016/j.probengmech.2020.103017
Received 20 January 2020; Accepted 27 January 2020
Available online 30 January 2020

white noise and filtered white noise excitations, possessing the commonly employed Tajimi–Kanai power spectral density (PSD), are considered for the horizontal ground acceleration. In this manner a combination of the statistical linearization, and of the static condensation approaches is employed to derive a computationally treatable equation governing the evolution of the rocking response statistics. The accuracy of the procedure is assessed via pertinent Monte Carlo simulation data using as model parameter values those obtained from previous experimental studies [31]. Finally, the survival probability related to toppling of blocks with different dynamic characteristics (geometry and foundation materials) is examined via Monte Carlo analyses. In this case, time-modulated filtered white noise excitations with PSD of the Tajimi–Kanai type are used to examine whether spectra with the same variance but different peak frequencies lead to variations of the survival probabilities of the blocks depending on their dynamic characteristics.

2. Mathematical formulation

Consider a rectangular rigid block with mass m, and polar moment of inertia I_{cm} about the center of mass cm, as shown in Fig. 1(a). The variable R denotes the distance of the base corners from the center of mass, situated at height h above the base of width $2b$. Further, let θ_{cr} be the critical tilt-angle, that is, the maximum angle to which the block can be tilted without overturning under the action of gravity, g, alone.

To simplify the ensuing analysis, the center of the base cb is restricted to vertical relative motion only [17]. Two generalized coordinates are employed to define the configuration of the block with respect to the foundation, as in Fig. 1(b). Specifically, the vertical displacement $z_{cb}(t)$ of the center of the base cb from the undeformed surface of the foundation (positive downward), and the rotation $\theta(t)$ of the block from its static equilibrium position (positive clockwise), are used. Further, if the foundation is exposed to a horizontal acceleration, $\ddot{x}_g(t)$, and vertical acceleration, $\ddot{z}_g(t)$, omitting henceforth the dependence from time t, the equations of motion are

$$m\ddot{z}_{cb} + mh\left(\dot{\theta}^2\cos\theta + \ddot{\theta}\sin\theta\right) + F_{cb} - mg = m\ddot{z}_g \tag{1}$$

and

$$\left(I_{cm} + mh^2\right)\ddot{\theta} + M_{cb} + mh\left(\ddot{z}_{cb} - g\right)\sin\theta = mh\left(\ddot{x}_g\cos\theta - \ddot{z}_g\sin\theta\right). \tag{2}$$

In these equations a dot over a variable denotes differentiation with respect to time, F_{cb} is the resultant vertical contact force, and M_{cb} is the induced moment of the contact force with respect to cb.

Eqs. (1) and (2) are the general equations of rocking when no sliding occurs. As it is apparent from these equations, the rocking phenomenon is strongly influenced by the kind of foundation considered, which is accounted for in the terms F_{cb} and M_{cb}. In this regard, the Winkler foundation model (WFM), that is a flexible foundation of distributed linear springs and dashpots, is widely used in literature [17]. Alternatively, a nonlinear foundation model can be employed. Specifically, following the approach in [29,31], it is reasonable to treat the foundation as a bed of continuously distributed and independent parallel springs and nonlinear dampers, with stiffness coefficient k (force units per unit width of base per unit vertical deformation), and damping coefficient λ (force units per unit width of base per unit vertical deformation velocity and per unit vertical deformation), respectively (Fig. 1(b)).

In this case, taking into account the possibility of uplifting condition occurring whenever one of the base corners (A or B) rises above the ground level, the impact/contact force F_{cb} and the moment M_{cb} in Eqs. (1), (2) can be expressed as

$$F_{cb} = 2bk\,z_{cb} + 2b\lambda\,z_{cb}\dot{z}_{cb} + \frac{2}{3}b^3\lambda\dot{\theta}\sin\theta\cos\theta, \tag{3}$$

and

$$M_{cb} = \frac{2}{3}b^3k\,\sin\theta\cos\theta + \frac{2}{3}b^3\lambda\dot{z}_{cb}\sin\theta\cos\theta + \frac{2}{3}b^3\lambda z_{cb}\dot{\theta}\cos^2\theta \tag{4}$$

for no-uplifting; while for uplifting condition (i.e. when $z_{cb} - b\sin|\theta| < 0$)

$$\begin{aligned} F_{cb} = {} & \frac{1}{2}b^2k\sin\theta\,\mathrm{sgn}\,\theta + k\,z_{cb}\left(b + \frac{1}{2}\frac{z_{cb}}{\sin\theta}\mathrm{sgn}\,\theta\right) + \frac{1}{2}b^2\lambda\,\dot{z}_{cb}\sin\theta\,\mathrm{sgn}\,\theta \\ & + \lambda z_{cb}\dot{z}_{cb}\left(b + \frac{1}{2}\frac{z_{cb}}{\sin\theta}\mathrm{sgn}\,\theta\right) + \frac{1}{3}b^3\lambda\dot{\theta}\cos\theta\sin\theta \\ & + \frac{1}{2}\lambda z_{cb}\dot{\theta}\cos\theta\times\left(b^2 - \frac{1}{3}\frac{z_{cb}^2}{\sin^2\theta}\right)\mathrm{sgn}\,\theta, \end{aligned} \tag{5}$$

and

$$\begin{aligned} M_{cb} = {} & \frac{b^3}{3}k\cos\theta\sin\theta + \frac{1}{2}k\,z_{cb}\cos\theta\left(b^2 - \frac{1}{3}\frac{z_{cb}^2}{\sin^2\theta}\right)\mathrm{sgn}\,\theta \\ & + \frac{b^3}{3}\lambda\dot{z}_{cb}\cos\theta\sin\theta + \frac{1}{4}b^4\lambda\dot{\theta}\sin\theta\cos^2\theta\,\mathrm{sgn}\,\theta \\ & + \frac{1}{2}\lambda z_{cb}\dot{z}_{cb}\cos\theta\left(b^2 - \frac{1}{3}\frac{z_{cb}^2}{\sin^2\theta}\right)\mathrm{sgn}\,\theta \\ & + \frac{1}{3}\lambda z_{cb}\dot{\theta}\cos^2\theta\left(b^3 + \frac{1}{4}\frac{z_{cb}^3}{\sin^3\theta}\mathrm{sgn}\,\theta\right), \end{aligned} \tag{6}$$

where $\mathrm{sgn}(\cdot)$ is the signum function returning the sign of its argument

2.1. Simplification

Eqs. (1) and (2) are coupled, piecewise and nonlinear. However, since θ and z_{cb} are small in most situations [17], good approximations can be obtained by assuming that $\sin\theta \approx \theta$, $\cos\theta \approx 1$ and neglecting all terms having combined derivative order of θ and z_{cb} greater than one. Assuming the ground excitation to be horizontal, i.e. $\ddot{z}_g = 0$, the equations for no uplifting become

$$m\ddot{z}_{cb} + 2b\lambda\,z_{cb}\dot{z}_{cb} + \frac{2}{3}b^3\lambda\theta\dot{\theta} + 2bkz_{cb} = mg \tag{7}$$

and

$$\left(I_c + mh^2\right)\ddot{\theta} + \frac{2}{3}b^3\lambda\dot{z}_{cb}\theta + \frac{2}{3}b^3\lambda z_{cb}\dot{\theta} + \frac{2}{3}b^3k\theta - mgh\theta = mh\,\ddot{x}_g; \tag{8}$$

while during uplifting become

$$\begin{aligned} & m\ddot{z}_{cb} + \lambda\,z_{cb}\dot{z}_{cb}\left(b + \frac{1}{2}\frac{z_{cb}}{\theta}\mathrm{sgn}\,\theta\right) + \frac{b^2}{2}\lambda\dot{z}_{cb}\theta\,\mathrm{sgn}\,\theta \\ & + \lambda z_{cb}\dot{\theta}\left[\frac{b^2}{2} - \frac{1}{6}\left(\frac{z_{cb}}{\theta}\right)^2\right]\mathrm{sgn}\,\theta + \frac{b^3}{3}\lambda\theta\dot{\theta} \\ & + \frac{b^2}{2}k\theta\,\mathrm{sgn}\,\theta + kz_{cb}\left(b + \frac{1}{2}\frac{z_{cb}}{\theta}\mathrm{sgn}\,\theta\right) = mg, \end{aligned} \tag{9}$$

and

$$\begin{aligned} & \left(I_c + mh^2\right)\ddot{\theta} + \frac{b^4}{4}\lambda\theta\dot{\theta}\,\mathrm{sgn}\,\theta + \frac{b^3}{3}\lambda\dot{z}_{cb}\theta + \lambda z_{cb}\dot{\theta}\left[\frac{b^3}{3} + \frac{1}{12}\left(\frac{z_{cb}}{\theta}\right)^3\mathrm{sgn}\,\theta\right] \\ & + \lambda z_{cb}\dot{z}_{cb}\left[\frac{b^2}{2} - \frac{1}{6}\left(\frac{z_{cb}}{\theta}\right)^2\right]\mathrm{sgn}\,\theta + \frac{b^3}{3}k\theta + kz_{cb}\left[\frac{b^2}{2} - \frac{1}{6}\left(\frac{z_{cb}}{\theta}\right)^2\right]\mathrm{sgn}\,\theta \\ & - mgh\theta = mh\,\ddot{x}_g\,. \end{aligned} \tag{10}$$

Further simplification of the problem can be achieved by applying the method of static condensation to Eqs. (7)–(10). In this manner, an explicit relationship between θ and z_{cb} is obtained satisfying Eqs. (7) and (9) under static conditions. Thus,

$$z_{cb} = z_{st} = \frac{mg}{2bk} \tag{11}$$

for no uplifting, and

$$z_{cb} = z_{st} = \frac{-bk\theta\,\mathrm{sgn}\,\theta + \sqrt{2mgk\theta\,\mathrm{sgn}\,\theta}}{2k} \tag{12}$$

for uplifting. Note that under static conditions uplifting occurs when $|\theta| > \theta_{ul}$, where

$$\theta_{ul} = \frac{|z_{st}|}{b} = \frac{mg}{2b^2k} \tag{13}$$

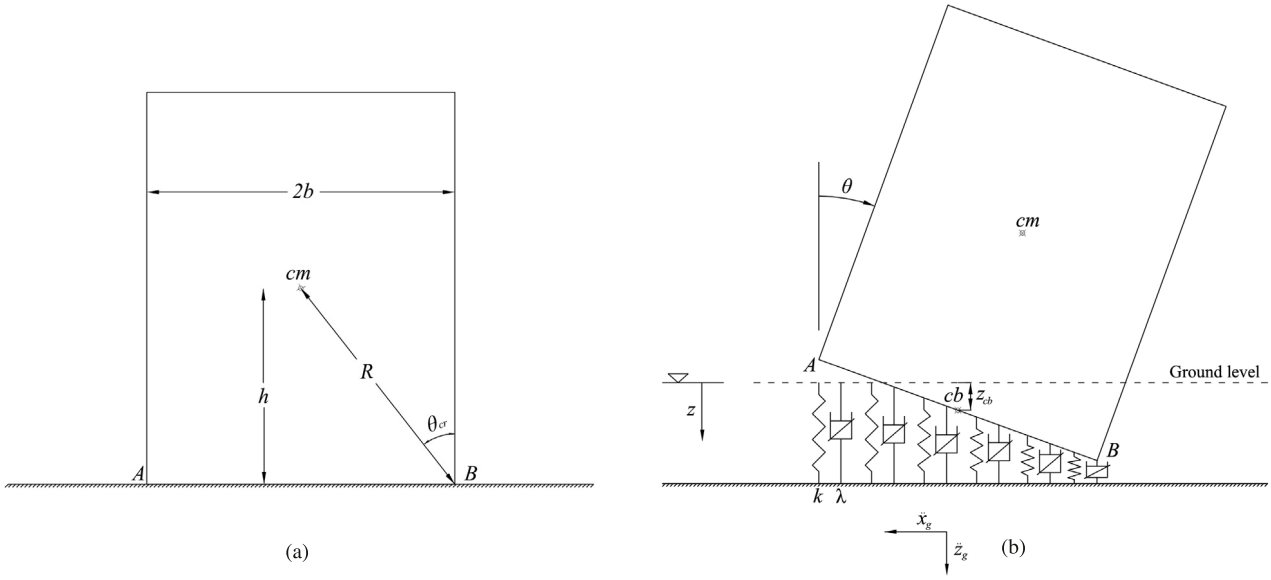

Fig. 1. (a) Block geometry; (b) Rocking block on nonlinear flexible foundation.

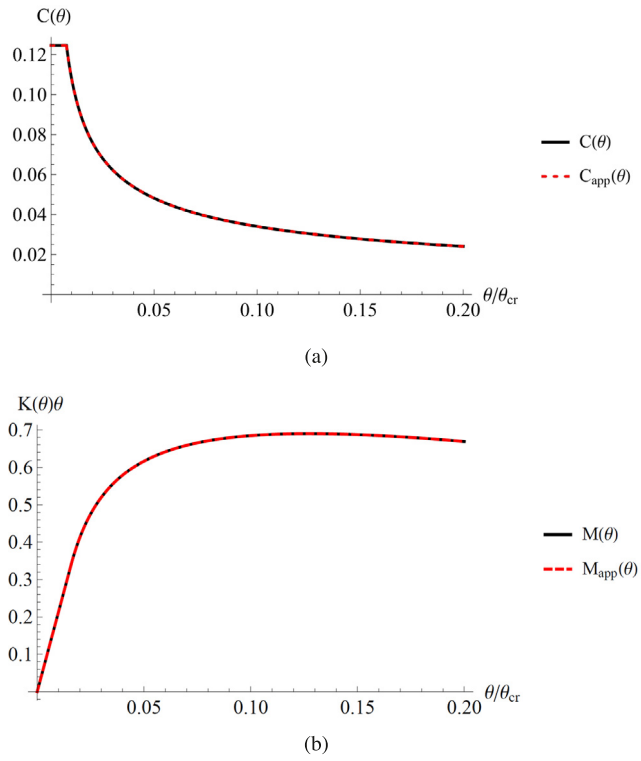

Fig. 2. Damping coefficient (a) and spring restoring moment (b), versus rotation angle.

Substituting Eqs. (11) and (12), Eqs. (8) and (9) become, respectively

$$\left(I_c + mh^2\right)\ddot{\theta} + \frac{b^2}{3}\lambda\frac{mg}{k}\dot{\theta} + \left(\frac{2}{3}b^3k - mgh\right)\theta = mh\,\ddot{x}_g, \tag{14}$$

and

$$\left(I_c + mh^2\right)\ddot{\theta} + \frac{mgb\lambda}{6k^2}\frac{\sqrt{2mgk\theta\operatorname{sgn}\theta}}{\theta}\dot{\theta}\operatorname{sgn}\theta + mg\left(\frac{b\operatorname{sgn}\theta}{\theta} - \frac{\sqrt{2mgk\theta\operatorname{sgn}\theta}}{3k\theta^2} - h\right)\theta = mh\,\ddot{x}_g. \tag{15}$$

Eqs. (14) and (15) can be recast in the form

$$m_{sdof}\ddot{\theta} + C(\theta)\dot{\theta} + K(\theta)\theta = mh\,\ddot{x}_g, \tag{16}$$

where the effective mass m_{sdof}, the variable damping coefficient $C(\theta)$ and the variable stiffness $K(\theta)$ are

$$m_{sdof} = \left(I_c + mh^2\right), \tag{17}$$

$$C(\theta) = \begin{cases} \dfrac{b^2}{3}\lambda\dfrac{mg}{k}; & |\theta| \le \theta_{ul} \\ \dfrac{mgb\lambda}{6k^2}\dfrac{\sqrt{2mgk\theta\operatorname{sgn}\theta}}{\theta}\operatorname{sgn}\theta; & |\theta| > \theta_{ul} \end{cases}, \tag{18}$$

and

$$K(\theta) = \begin{cases} \dfrac{2}{3}b^3k - mgh; & |\theta| \le \theta_{ul} \\ mg\left(\dfrac{b\operatorname{sgn}\theta}{\theta} - \dfrac{\sqrt{2mgk\theta\operatorname{sgn}\theta}}{3k\theta^2} - h\right); & |\theta| > \theta_{ul} \end{cases} \tag{19}$$

Note that Eq. (16) represents a single degree of freedom system which is linear for $|\theta| \le \theta_{ul}$.

3. Stochastic linearization

Let the horizontal ground acceleration be modeled as a time-modulated random excitation. That is,

$$\ddot{x}_g = q(t)\,v(t), \tag{20}$$

where $v(t)$ is a stationary broad-band random process with double-sided power spectral density (PSD) $S_v(\omega)$, and $q(t)$ is a deterministic function used to capture the typical intensity variation of classical earthquake records. Next, the method of stochastic linearization can be applied to estimate block response to moderate level random base excitation. To this end, firstly the piecewise variable damping coefficient $C(\theta)$ is rewritten as

$$C_{app}(\theta) = f(\theta)\,C_1(\theta) + [1 - f(\theta)]\,C_2(\theta), \tag{21}$$

where $C_1(\theta) = C(\theta)$ for $|\theta| \le \theta_{ul}$, $C_2(\theta) = C(\theta)$ for $|\theta| > \theta_{ul}$ in Eq. (18), and $f(\theta)$ is

$$f(\theta) = U\left(\theta + \theta_{ul}\right) - U\left(\theta - \theta_{ul}\right), \tag{22}$$

where $U(\cdot)$ is the unit-step function.

Similarly, the piecewise spring restoring moment $M(\theta) = K(\theta)\theta$ is rewritten as

$$M_{app}(\theta) = \left\{f(\theta)\,K_1(\theta) + [1 - f(\theta)]\,K_2(\theta)\right\}\theta, \tag{23}$$

where

$$K_1(\theta) = K(\theta) \quad for \quad |\theta| \le \theta_{ul}$$
$$K_2(\theta) = K(\theta) \quad for \quad |\theta| > \theta_{ul} \tag{24}$$

Fig. 2 shows the approximated damping and spring restoring moment Eqs. (21), (23), vis-à-vis the corresponding exact expressions Eqs. (18), (19).

Further, substituting Eqs. (20), (21) and (23) into Eq. (16) yields

$$m_{sdof}\ddot{\theta} + C_{app}(\theta)\dot{\theta} + M_{app}(\theta) = mh\,q(t)\,v(t), \tag{25}$$

which is a convenient approximate version of the equation of motion of the rocking block Eq. (16).

Applying the method of stochastic linearization on Eq. (25), an equivalent linear system can be introduced as

$$m_{sdof}\ddot{\theta} + c_e\dot{\theta} + k_e\theta = mh\,q(t)\,v(t), \tag{26}$$

where c_e and k_e are the equivalent linear damping and stiffness coefficients, respectively. Following [29,33], these terms can be determined by the equations

$$c_e = \mathrm{E}\left[\frac{\partial g(\theta,\dot{\theta})}{\partial\dot{\theta}}\right], \tag{27}$$

and

$$k_e = \mathrm{E}\left[\frac{\partial g(\theta,\dot{\theta})}{\partial\theta}\right], \tag{28}$$

where $\mathrm{E}[\cdot]$ is the mathematical expectation operator, and

$$g(\theta,\dot{\theta}) = C_{app}(\theta)\dot{\theta} + M_{app}(\theta) = \left\{f(\theta)C_1(\theta) + [1-f(\theta)]C_2(\theta)\right\}\dot{\theta} + \left\{f(\theta)K_1(\theta) + [1-f(\theta)]K_2(\theta)\right\}\theta \tag{29}$$

Considering that θ and $\dot{\theta}$ can be approximated as Gaussian processes, the joint probability density function is given by the equation

$$p_{\theta\dot{\theta}} = \frac{1}{2\pi\sigma_\theta\sigma_{\dot{\theta}}\sqrt{1-\rho^2}}\exp\left[\frac{-\left(\sigma_{\dot{\theta}}^2\theta^2 - 2\sigma_\theta\sigma_{\dot{\theta}}\rho\theta\dot{\theta} + \sigma_\theta^2\dot{\theta}^2\right)}{2\sigma_\theta^2\sigma_{\dot{\theta}}^2}\right], \tag{30}$$

where σ_θ and $\sigma_{\dot{\theta}}$ are the standard deviations of θ and $\dot{\theta}$, respectively; ρ is their correlation coefficient. In this manner, the expectation in Eqs. (27) and (28) can be evaluated leading to the equivalent damping and stiffness coefficients

$$c_e = \frac{b^2gm\lambda}{3k}\mathrm{erf}\left(\frac{\theta_{ul}}{\sqrt{2}\sigma_\theta}\right) + bgm\sqrt{gmk}\frac{\lambda\sqrt{\theta_{ul}}}{6k^2\sqrt{\pi}\sigma_\theta}E_{3/4}\left(\frac{\theta_{ul}^2}{2\sigma_\theta^2}\right), \tag{31}$$

and

$$k_e = -mgh + \frac{b}{3\sigma_\theta}\sqrt{\frac{2}{\pi}}\exp\left(-\frac{\theta_{ul}^2}{2\sigma_\theta^2}\right)\left(3gm - 2b^2k\theta ul\right) + \frac{2}{3}b^3\mathrm{erf}\left(\frac{\theta_{ul}}{\sqrt{2}\sigma_\theta}\right) - \frac{1}{6}\frac{gm}{k\sqrt{\pi}\sigma_\theta^3}E_{1/4}\left(\frac{\theta_{ul}^2}{2\sigma_\theta^2}\right)\left[\theta_{ul}\sqrt{gmk\theta_{ul}} + \left(\frac{\theta_{ul}^2}{\sigma_\theta^2}\right)^{\frac{3}{4}}\sigma_\theta\sqrt{gmk\sigma_\theta}\right] - \frac{1}{24}\frac{bgm}{k^2\sqrt{\pi}}\lambda\rho\frac{\sigma_{\dot{\theta}}}{\sigma_\theta^2}E_{3/4}\left(\frac{\theta_{ul}^2}{2\sigma_\theta^2}\right)\left[\left(\frac{\theta_{ul}^2}{\sigma_\theta^2}\right)^{\frac{1}{4}}\sqrt{gmk\sigma_\theta} + \sqrt{gmk\theta_{ul}}\right] + \frac{bgm}{3k^2\sqrt{\pi}}\lambda\rho\frac{\sigma_{\dot{\theta}}}{\sigma_\theta^2}\exp\left(-\frac{\theta_{ul}^2}{2\sigma_\theta^2}\right)\left(\sqrt{gmk\theta_{ul}} - \sqrt{2}bk\theta_{ul}\right). \tag{32}$$

Note that in Eqs. (31) and (32) the term $E_{3/4}\left(\frac{\theta_{ul}^2}{2\sigma_\theta^2}\right)$ is the so-called exponential integral function $E_n(x)$ of order $n = 3/4$, defined as [34]

$$E_n(x) = \int_1^\infty \frac{\exp(-sx)}{s^n}ds \tag{33}$$

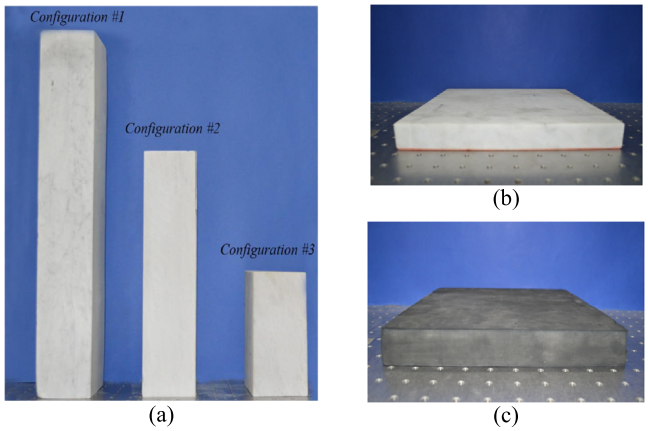

Fig. 3. Blocks and base foundation: (a) Marble block configurations; (b) Rigid base (marble material); (c) Soft base (Aerstop CN20 material).

Table 1
Marble blocks configuration parameters.

	Configuration #1	Configuration #2	Configuration #3
$2h$	0.42 m	0.28 m	0.14 m
$2b$	0.07 m	0.07 m	0.07 m
h/b	6	4	2
m	8.67 kg	5.84 kg	2.98 kg
θ_{cr}	9.46°	14°	26.56°

Table 2
Nonlinear foundation model parameters.

	Configuration #1		Configuration #2		Configuration #3	
	k	λ	k	λ	k	λ
Marble foundation	$2.89\cdot10^7$	$8.95\cdot10^8$	$6.88\cdot10^6$	$1.3\cdot10^8$	$6.42\cdot10^6$	$1.65\cdot10^8$
Aerstop CN20 foundation	$3.16\cdot10^6$	$2.16\cdot10^8$	$2.86\cdot10^6$	$8.16\cdot10^7$	$1.47\cdot10^6$	$1.41\cdot10^7$

As it can be seen, these expressions are quite different from those obtained in [29] for the WFM. This is due to the fact that both a different foundation model, and different approximate damping and restoring moment coefficients $C_{app}(\theta)$, $M_{app}(\theta)$ have been used.

3.1. Solution procedure for modulated white noise excitation

Let $v(t)$ in Eq. (20) be a stationary white noise $w(t)$ with constant PSD S_0. Using standard approaches for linear system under white noise excitation, the stochastic response of the equivalent linear system Eq. (26) can be determined employing the so-called Lyapunov equation for the evolution of the covariance matrix. In this regard, Eq. (26) can be conveniently rewritten in state space notation as

$$\dot{\mathbf{u}} = \mathbf{P}\mathbf{u} + \mathbf{v}, \tag{34}$$

where

$$\mathbf{u} = \begin{bmatrix}\theta(t)\\ \dot{\theta}(t)\end{bmatrix}, \tag{35}$$

$$\mathbf{P} = \begin{bmatrix}0 & 1\\ -k_e/m_{sdof} & -c_e/m_{sdof}\end{bmatrix}, \tag{36}$$

and

$$\mathbf{v} = \begin{bmatrix}0\\ mh\,q(t)w(t)/m_{sdof}\end{bmatrix} \tag{37}$$

Further, introducing the covariance matrix

$$\mathbf{C} = \begin{bmatrix}\sigma_\theta^2 & \sigma_{\theta\dot{\theta}}\\ \sigma_{\theta\dot{\theta}} & \sigma_{\dot{\theta}}^2\end{bmatrix}, \tag{38}$$

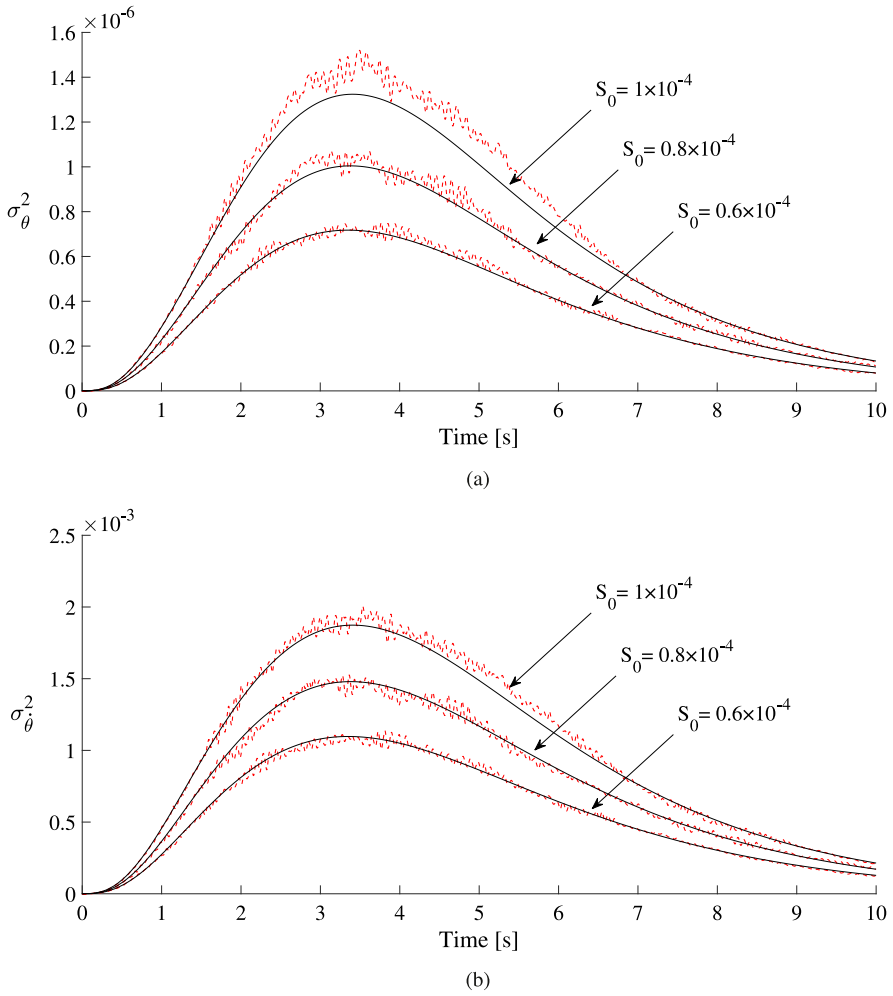

Fig. 4. Configuration #1 on Marble foundation: (a) Rotation angle variance; (b) Angular velocity variance. Stochastic averaging-black lines; MCS-red dashed lines.

where $\sigma_{\theta\dot{\theta}} = \rho\,\sigma_\theta\,\sigma_{\dot{\theta}}$, its evolution is governed by the Lyapunov equation as

$$\dot{\mathbf{C}} = \mathbf{PC} + \mathbf{CP}^T + E\left[\mathbf{vv}^T\right], \tag{39}$$

where

$$E\left[\mathbf{vv}^T\right] = \begin{bmatrix} 0 & 0 \\ 0 & 2\pi S_0 \left(mhq(t)/m_{sdof}\right)^2 \end{bmatrix} \tag{40}$$

Note that Eq. (39) is nonlinear. Thus, a numerical integration procedure is required to determine the evolution of the variances σ_θ^2 and $\sigma_{\dot{\theta}}^2$.

3.2. Solution procedure for modulated filtered white noise excitation

Next, let $v(t)$ in Eq. (20) be a filtered white noise process. Specifically, adopting for example the well-known Tajimi–Kanai filtered process, commonly utilized in earthquake engineering applications, $v(t)$ can be expresses as

$$v(t) = -2\zeta_g\omega_g\dot{u}_g - \omega_g^2 u_g, \tag{41}$$

where $u_g(t)$ is the response of the equation of the filter

$$\ddot{u}_g + 2\zeta_g\omega_g\dot{u}_g + \omega_g^2 u_g = w(t), \tag{42}$$

in which ω_g and ζ_g are the soil natural frequency and damping ratio, respectively, and $w(t)$ is a white noise process with constant PSD S_0.

Note that, the PSD $S_v(\omega)$ of the process $v(t)$ *is*

$$S_v(\omega) = S_0 \frac{4\zeta_g^2\omega_g^2\omega^2 + \omega_g^4}{\left(\omega_g^2 - \omega^2\right)^2 + 4\zeta_g^2\omega_g^2\omega^2}, \tag{43}$$

In this manner, the stochastic response of the equivalent linear system Eq. (26) can be determined again by resorting to the Lyapunov equation for the evolution of the covariance matrix. In this regard, taking into account Eqs. (41) and (42), the state space notation in Eq. (34) of the equivalent linear system Eq. (26) can be utilized, where in this case

$$\mathbf{u} = \begin{bmatrix} \theta(t) \\ \dot{\theta}(t) \\ u_g(t) \\ \dot{u}_g(t) \end{bmatrix}, \tag{44}$$

$$\mathbf{P} = \begin{bmatrix} 0 & 1 & 0 & 0 \\ -\dfrac{k_e}{m_{sdof}} & -\dfrac{c_e}{m_{sdof}} & -q(t)\dfrac{mh\omega_g^2}{m_{sdof}} & -q(t)\dfrac{2mh\zeta_g\omega_g}{m_{sdof}} \\ 0 & 0 & 0 & 1 \\ 0 & 0 & -\omega_g^2 & -2\zeta_g\omega_g \end{bmatrix}, \tag{45}$$

and

$$\mathbf{v} = \begin{bmatrix} 0 \\ 0 \\ 0 \\ w(t) \end{bmatrix} \tag{46}$$

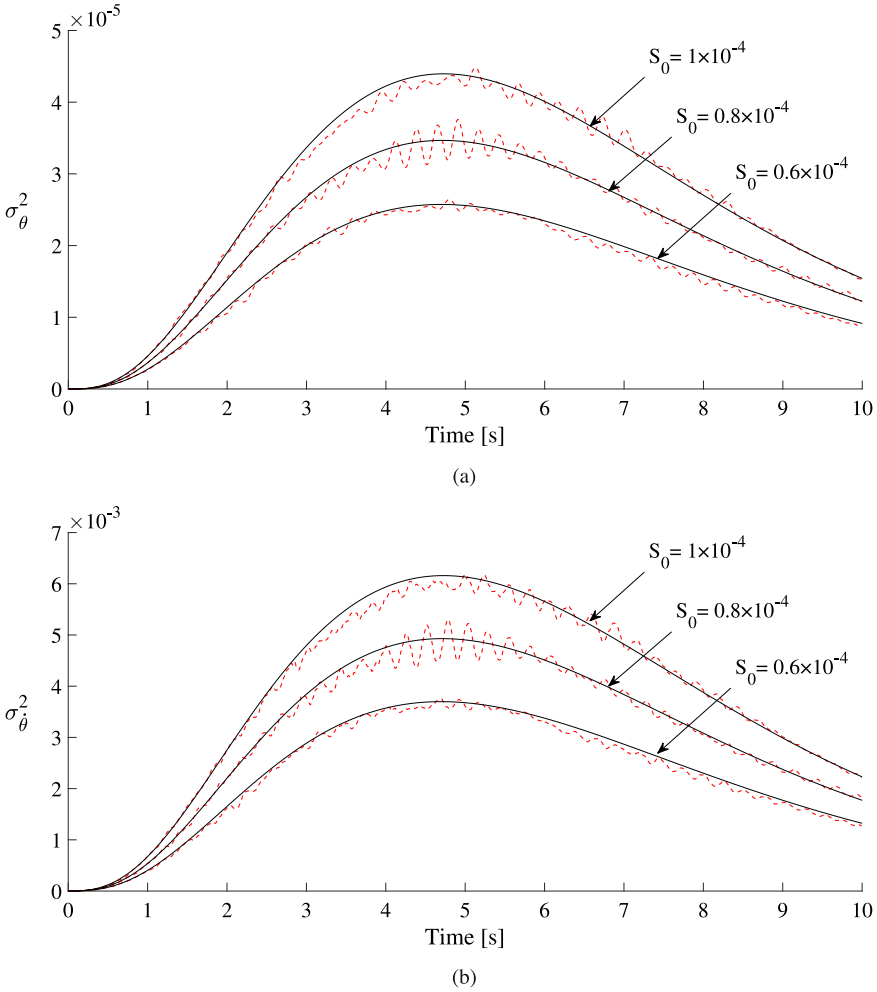

Fig. 5. Configuration #1 on Aerstop CN20 foundation: (a) Rotation angle variance; (b) Angular velocity variance. Stochastic averaging-black lines; MCS-red dashed lines.

Next, introducing the covariance matrix

$$\mathbf{C} = \begin{bmatrix} \sigma_\theta^2 & \sigma_{\theta\dot\theta} & \sigma_{\theta u_g} & \sigma_{\theta\dot u_g} \\ \sigma_{\theta\dot\theta} & \sigma_{\dot\theta}^2 & \sigma_{\dot\theta u_g} & \sigma_{\dot\theta\dot u_g} \\ \sigma_{\theta u_g} & \sigma_{\dot\theta u_g}^2 & \sigma_{u_g}^2 & \sigma_{u_g\dot u_g}^2 \\ \sigma_{\theta\dot u_g} & \sigma_{\dot\theta\dot u_g}^2 & \sigma_{u_g\dot u_g}^2 & \sigma_{\dot u_g}^2 \end{bmatrix}, \tag{47}$$

its evolution is governed by the Lyapunov equation as

$$\dot{\mathbf{C}} = \mathbf{P}\mathbf{C} + \mathbf{C}\mathbf{P}^T + E\left[\mathbf{v}\mathbf{v}^T\right], \tag{48}$$

where

$$E\left[\mathbf{v}\mathbf{v}^T\right] = \begin{bmatrix} 0 & 0 & 0 & 0 \\ 0 & 0 & 0 & 0 \\ 0 & 0 & 0 & 0 \\ 0 & 0 & 0 & 2\pi S_0 \end{bmatrix} \tag{49}$$

Again, note that Eq. (48) is nonlinear, and a numerical integration procedure is required to determine the evolution of the sought variances σ_θ^2 and $\sigma_{\dot\theta}^2$.

4. Numerical results

In this section the proposed approach is applied to the case of rigid blocks on nonlinear foundation model considering both the cases of time-modulated white noise, and filtered white noise excitation employing the modulating function [35]

$$q(t) = 4\left[\exp\left(-\frac{t}{4}\right) - \exp\left(-\frac{t}{2}\right)\right], \tag{50}$$

which rises rapidly from zero to a unitary peak and then decays exponentially to zero.

To assess the accuracy of the proposed procedure, stochastic linearization based statistical moments are juxtaposed with the results of pertinent Monte Carlo simulations (MCS) data, obtained by numerically integrating the original nonlinear equations of motion Eqs. (1)–(6). Analyses have been carried out using as parameter values those obtained from the experimental studies in [31]. In this regard, three different marble block configurations (Fig. 3(a)), and two different base materials (Fig. 3(b–c)) have been considered to investigate the influence of block geometries, and foundation material. Specifically, rigid and soft foundations material have been assumed using a marble slab and a pad made of Aerstop CN20 material, respectively. Pertinent parameters involved in the equations, as determined in [31], are reported in Tables 1 and 2.

Note that for each case several values of the PSD of the white noise S_0 have been used, which result in uplifting, but no toppling, of the blocks. Further, quiescent initial conditions have been assumed, and 2000 samples have been used for each MCS.

As far as the case of time-modulated white noise excitation is concerned, as discussed in Section 3.1, response variances of the proposed approach (black lines) for Configuration #1, determined solving Eq. (39), are plotted in Figs. 4 and 5 vis-à-vis pertinent MCS results (red dashed lines). Specifically, in these figures results for rigid marble block foundation (Fig. 4) and soft foundation made of Aerstop CN20 material (Fig. 5) are considered. As it can be seen, the proposed procedure results agree reasonably well with the MCS data for all the chosen values of S_0.

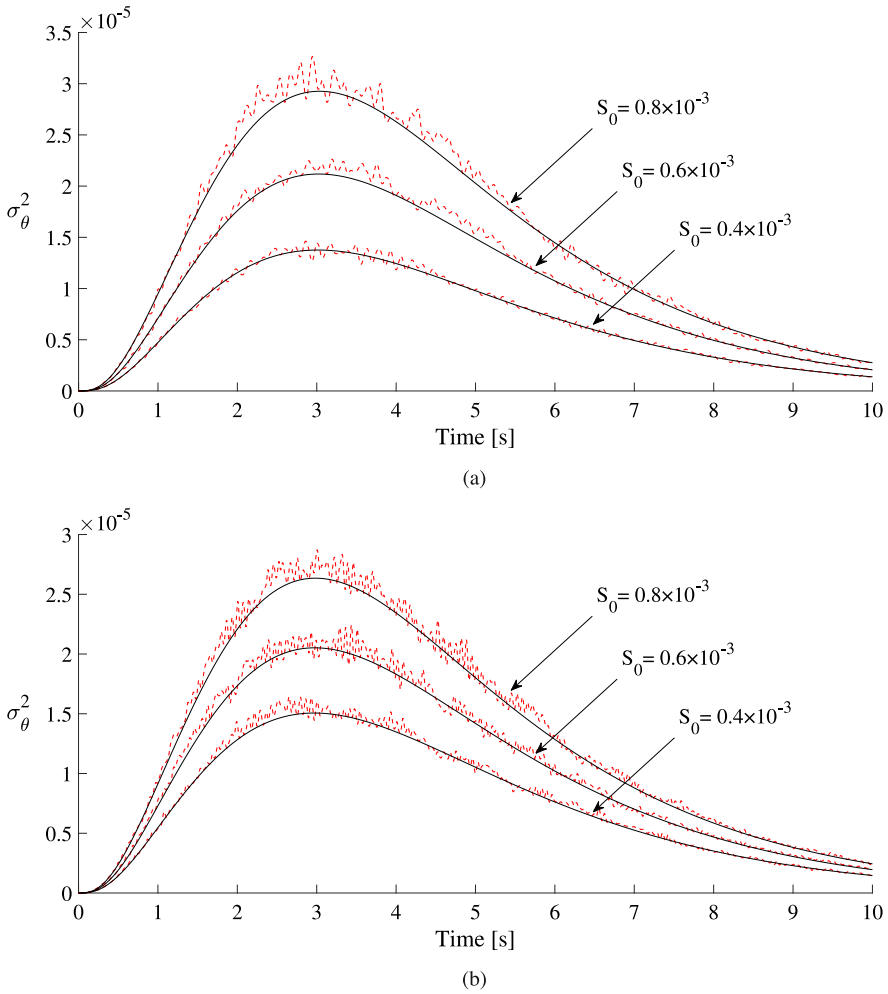

Fig. 6. Rotation angle variances for Aerstop-CN20 foundation: (a) Configuration #2; (b) Configuration #3. Stochastic averaging-black lines; MCS-red dashed lines.

Further, analyses for Configurations #2 and #3 are captured in Fig. 6, considering as foundation the Aerstop-CN20 material. As it can be seen, again the MCS data (red dashed lines) are in good agreement with the results of the proposed approach (black lines) for all the values of S_0.

As far as the case of a horizontal ground excitation modeled as a time-modulated filtered white noise process is concerned, response variances of the proposed approach (black lines) for Configurations #2 and #3, determined solving Eq. (48), are plotted in Fig. 7 vis-à-vis pertinent MCS results (red dashed lines) considering the soft foundation made of Aerstop CN20 material. Note that, for these analyses three different values of the PSD of the white noise S_0 have been used, causing uplifting, but no toppling, of the blocks, while $\omega_g = 10$ rad/s, and $\zeta_g = 0.4$ have been employed as soil parameters in Eqs. (41)–(43).

As it can be seen in these figure, again the MCS data are in a quite good agreement with the results of the proposed approach for all the values of S_0, especially for Configuration #3.

4.1. Survival probability of the blocks

Next, proceed to investigate the response of the blocks to excitations which are strong enough to cause toppling. Specifically, hereinafter the horizontal random excitation is modeled as a time-modulated filtered white noise process as in Eqs. (41)–(43), and a power spectrum of the Tajimi–Kanai type is assumed. To examine the response of blocks with different dynamic characteristics (geometric features and foundation materials), the probability that the blocks will not topple in a prescribed time frame, i.e. the survival probability of the blocks, is examined. To this aim MCS analyses have been performed solving the original nonlinear differential equations Eqs. (1)–(6).

Note that, the PSD $S_v(\omega)$ of the form given in Eq. (43) is used to generate the samples of the stationary random process, using different typical values of the natural frequency ω_g and damping ratio ζ_g of the soil. For each set of soil parameters ω_g and ζ_g, pertinent value of S_0 is used in Eq. (43), so as to keep constant the variance of $S_v(\omega)$. In this manner, it is possible to examine whether spectra with the same variance but different peak frequencies lead to variations of the survival probabilities of the blocks depending on their dynamic characteristics.

In this regard Fig. 8 shows the PSDs given in Eq. (43) for three typical values of ω_g, and pertinent values of S_0 employed in the numerical analyses.

Further, Fig. 9 shows a comparison among the survival probabilities of the block Configuration #1 and #2, considering the Aerstop-CN20 foundation material. As it can be seen, the geometric features of the blocks influence strongly the survival probability of toppling, for all the values of ω_g used for the PSD $S_v(\omega)$. Further, Configuration #1 appears to be much more prone to toppling than Configuration #2; and this is perhaps due to the fact that the critical angle θ_{cr} of the block Configuration #1 is much smaller than the corresponding one for Configuration #2, as also shown in Table 1. However, while higher survival probability for Configuration #2 is reached for $\omega_g = 5$ rad/s, this value of soil natural frequency leads to the lowest survival probability for Configuration #1. Therefore, the peak natural frequency also influences the toppling response of the blocks.

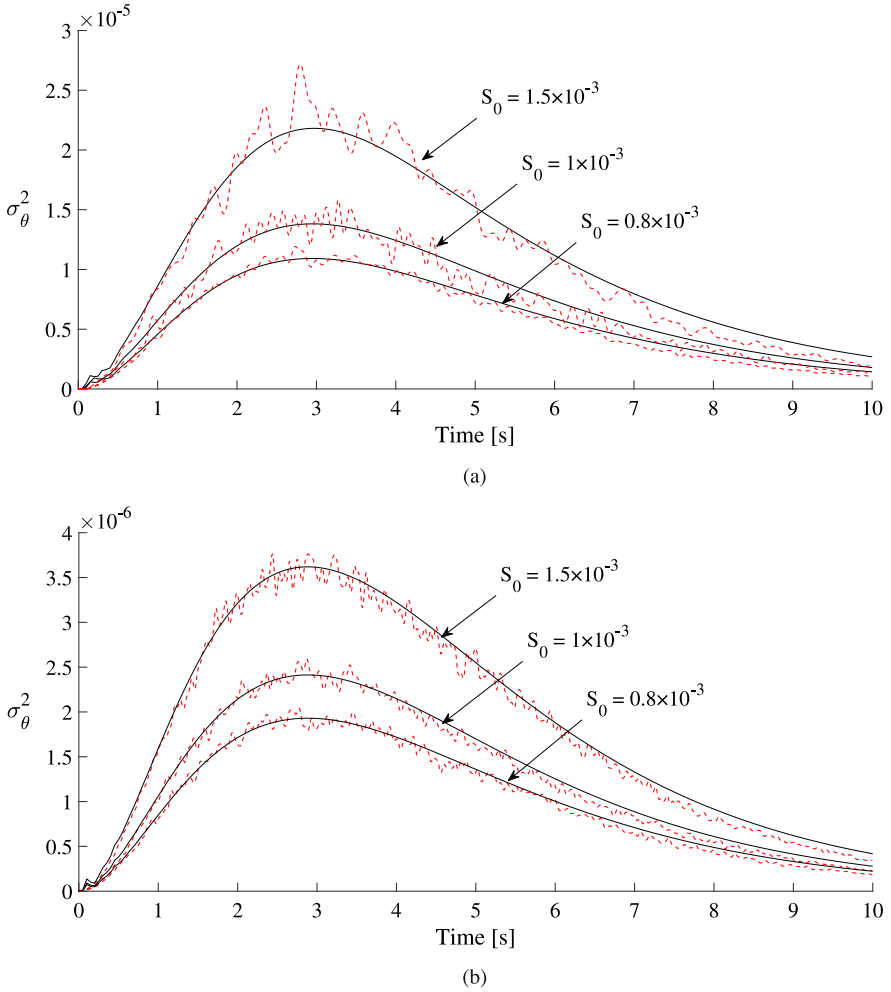

Fig. 7. Rotation angle variances for Aerstop-CN20 foundation: (a) Configuration #2; (b) Configuration #3. Stochastic averaging-black lines; MCS-red dashed lines.

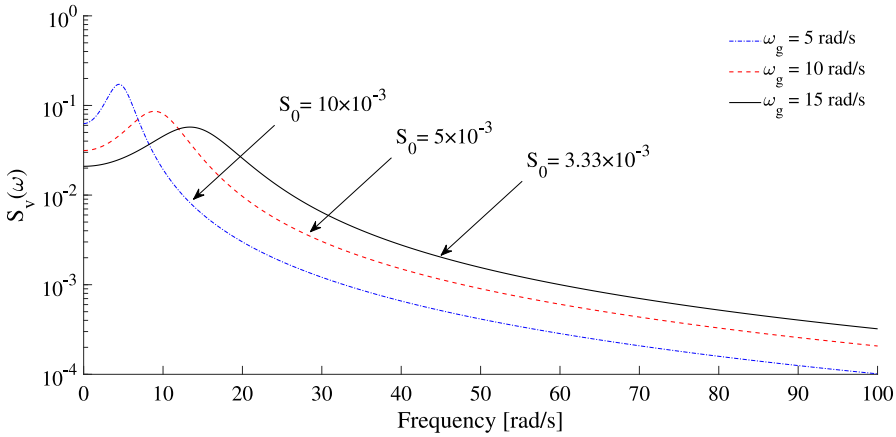

Fig. 8. Power spectral density of the Tajimi–Kanai type for different soil natural frequency.

Similar analysis has been also carried out considering an identical block configuration but different foundation materials. In this regard Fig. 10 shows a comparison among the survival probabilities of the block Configuration #2, using the rigid marble foundation and the soft Aerstop-CN20 foundation materials.

As it can be seen in this figure, the survival probability of the block is also strongly influenced by the foundation material employed, leading to very different behavior for the same peak natural frequency of the soil. Specifically, lowest survival probability is reached in the case of marble foundation with $\omega_g = 15$ rad/s, while the corresponding one for Aerstop-CN20 foundation is much higher. Thus, a soft foundation material could be beneficial for avoiding toppling of blocks with geometrical properties of Configuration #2 in area characterized by that value of soil natural frequency. On the other hand, as it can be seen in Fig. 10, the marble foundation leads also to the highest survival

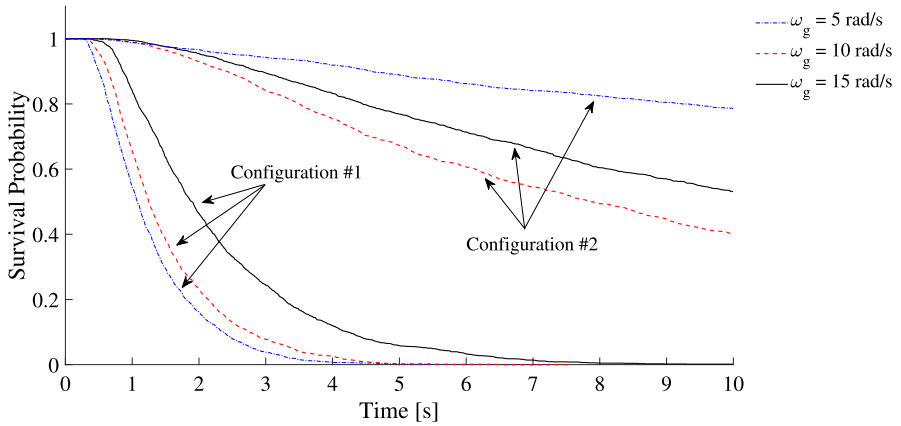

Fig. 9. Survival probability for Configuration #1 and #2 on Aerstop-CN20 foundation material.

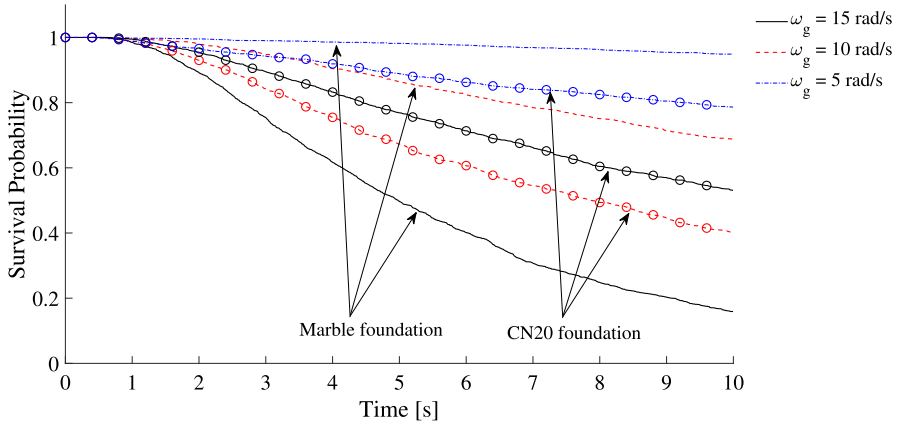

Fig. 10. Survival probability for Configuration #2 on Marble foundation (lines) and Aerstop-CN20 foundation material (lines with circles).

probability, considering a soil with $\omega_g = 5$ rad/s. Thus, in this case the soft foundation shows a detrimental counterintuitive effect.

Concluding Remarks

The behavior of a rigid block resting on a flexible foundation and subjected to a random horizontal shacking has been investigated. For this purpose, a versatile nonlinear model of the foundation has been used. The original two piecewise coupled nonlinear equations of motion have been reduced to one through a static condensation scheme. Specifically, appropriate analytical functions have been used to approximate the piecewise continuous damping and restoring moment. Further, modeling the excitation as a time-modulated white noise and filtered white noise, the stochastic linearization has been used to determine the evolution of the rotation angle and angular velocity variances. Several numerical Monte Carlo simulations have been carried out considering various model parameters selected using pertinent experimental data, for different kinds of block geometries and foundation materials. The Monte Carlo data have demonstrated the reasonable efficiency and reliability of the proposed method. Finally, the survival probability to toppling of blocks with different dynamic characteristics (geometry and foundation materials) has been examined by Monte Carlo studies. Time-modulated filtered white noise excitations possessing a power spectrum of the Tajimi–Kanai type have been used considering spectra with the same variance but with different peak frequencies. In this manner, it has been shown that the probability of toppling of the blocks depends not only on the block geometry and foundation material, but also on the soil dynamic parameters which characterize the random base excitation, hence leading in some cases also to counterintuitive responses. Thus, if the choice of a foundation material is of interest for protecting a block from toppling, a thorough numerical analysis, as the one performed herein, should be carried out to assess properly the probability of toppling of that specific block.

References

[1] G.W. Housner, The behavior of inverted pendulum structures during earthquakes, Bull. Seismol. Soc. Am. 53 (1963) 403–417.
[2] M. Aslam, W.G. Godden, D.T. Scalise, Earthquake rocking response of rigid bodies, J. Struct. Div. 106 (1980) 377–392.
[3] D. Konstantinidis, N. Makris, Experimental and analytical studies on the response of freestanding laboratory equipment to earthquake shaking, Earthq. Eng. Struct. Dyn. 38 (2009) 827–848.
[4] M.S. Agbabian, W.S. Ginell, F.S. Masri, R.L. Nigbor, Evaluation of earthquake damage mitigation methods for museum objects, Stud. Conserv. 36 (1991) 111–120.
[5] A.N. Kounadis, On the rocking complex response of ancient multispondyle columns: a genious and challenging structural system requiring reliable solution, Meccanica 50 (2015) 261–292.
[6] A.N. Kounadis, Seismic instability of free-standing statues atop multispondyle columns: A heuristic very stable system of ancient technology, Soil Dyn. Earthq. Eng. 119 (2019) 253–264.
[7] C.S. Yim, A.K. Chopra, J. Penzien, Rocking response of rigid blocks to earthquakes, Earthq. Eng. Struct. Dyn. 8 (1980) 565–587.
[8] A.S. Koh, C.M. Hsiung, Base isolation benefits of 3-D rocking and uplift I: theory, J. Eng. Mech. 117 (1991) 1–18.
[9] E. Ahmadi, M.M. Kashani, On the use of entangled wire materials in pre-tensioned rocking columns, J. Phys. Conf. Ser. 1264 (2019) 012007.
[10] A. Palmeri, N. Makris, Response of rigid structures rocking on viscoelastic foundation, Earthq. Eng. Struct. Dyn. 37 (2008) 1039–1063.
[11] A. Gesualdo, A. Iannuzzo, V. Minutolo, M. Monaco, Rocking of freestanding objects: theoretical and experimental comparisons, J. Theoret. Appl. Mech. 56 (2018) 977–991.
[12] P.D. Spanos, P.C. Roussis, N.P.A. Politis, Dynamic analysis of stacked rigid blocks, Soil Dyn. Earthq. Eng. 21 (2001) 559–579.

[13] S. Lenci, G. Rega, A dynamical systems approach to the overturning of rocking blocks, Chaos Solitons Fractals 28 (2006) 527–542.
[14] S.C.S. Yim, H. Lin, Nonlinear impact and chaotic response of slender rocking objects, J. Eng. Mech. 117 (1991) 2079–2100.
[15] E.G. Dimitrakopoulos, M.J. DeJong, Revisiting the rocking block: closed-form solutions and similarity laws, Proc. R. Soc. Lond. Ser. A Math. Phys. Eng. Sci. 468 (2012) 2294–2318.
[16] P.D. Spanos, A.S. Koh, Rocking of rigid blocks due to harmonic shaking, J. Eng. Mech. 110 (1984) 1627–1642.
[17] A.S. Koh, P.D. Spanos, J.M. Roesset, Harmonic rocking of rigid block on flexible foundation, J. Eng. Mech. 112 (1986) 1165–1180.
[18] I.N. Psycharis, P.C. Jennings, Rocking of slender rigid bodies allowed to uplift, Earthq. Eng. Struct. Dyn. 11 (1983) 57–76.
[19] S.C.S. Yim, A.K. Chopra, Earthquake response of structures with partial uplift on Winkler foundation, Earthq. Eng. Struct. Dyn. 12 (1984) 263–281.
[20] M.N. Chatzis, A.W. Smyth, Robust modeling of the rocking problem, J. Eng. Mech. 138 (2012) 247–262.
[21] R.N. Iyengar, C.S. Manohar, Rocking response of rectangular rigid blocks under random noise base excitations, Int. J. Non-Linear Mech. 26 (1991) 885–892.
[22] M.F. Dimentberg, Y.K. Lin, R. Zhang, Toppling of computer-type equipment under base excitation, J. Eng. Mech. 119 (1991) 145–160.
[23] H. Lin, S.C.S. Yim, Deterministic and stochastic analyses of chaotic and overturning responses of a slender rocking object, Nonlinear Dynam. 11 (1996) 83–106.
[24] H. Lin, S.C.S. Yim, Nonlinear rocking motions II: overturning under random excitations, J. Eng. Mech. 122 (1996) 728–735.
[25] A. Kovaleva, The melnikov criterion of instability for random rocking dynamics of rigid block with an attached secondary structure, Nonlinear Anal. Real World Appl. 11 (2010) 472–479.
[26] A. Kovaleva, Random rocking dynamics of a multidimensional structure, in: R.A. Ibrahim, V.I. Babitsky, M. Okuma (Eds.), Vibro-Impact Dynamics of Ocean Systems and Related Problems, in: Lecture Notes in Applied and Computational Mechanics, vol. 44, Springer, Berlin.
[27] A. Kovaleva, Stability and control of random rocking motion of a multi-dimensional structure: the Melnikov approach, Nonlinear Dynam. 59 (2010) 309–317.
[28] P.D. Spanos, A.S. Koh, Analysis of block random rocking, Soil Dyn. Earthq. Eng. 5 (1986) 178–183.
[29] A.S. Koh, Rocking of rigid blocks on randomly shaking foundations, Nucl. Eng. Des. 97 (1986) 269–276.
[30] M.A. ElGawady, Q. Ma, J.W. Butterworth, J. Ingham, Effects of interface material on the performance of free rocking blocks, Earthq. Eng. Struct. Dyn. 40 (2011) 375–392.
[31] P.D. Spanos, A. Di Matteo, A. Pirrotta, M. Di Paola, Rocking of rigid block on nonlinear flexible foundation, Int. J. Non-Linear Mech. 94 (2017) 362–374.
[32] K.H. Hunt, F.R.E. Crossley, Coefficient of restitution interpreted as damping in vibroimpact, J. Appl. Mech. 42 (1975) 440–445.
[33] J.B. Roberts, P.D. Spanos, Random Vibration and Statistical Linearization, Dover Publications, New York, 2003.
[34] M. Abramowitz, J. Stegun, Handbook of Mathematical Functions with Formulas, Graphs and Mathematical Tables, Dover Publications, New York, USA, 1963.
[35] M. Shinozuka, Y. Sato, Simulation of nonstationary random process, ASCE J. Eng. Mech. Div. 93 (1967) 11–40.